Molecular Biology of the Cell
Vol. 21, 3070–3079, September 1, 2010

Differential Requirements for Clathrin-dependent Endocytosis at Sites of Cell–Substrate Adhesion

Erika M. Batchelder and Defne Yarar

The Whitehead Institute for Biomedical Research and the Koch Institute for Integrative Cancer Research, Cambridge, MA 02142

Submitted December 16, 2009; Revised June 29, 2010; Accepted July 7, 2010
Monitoring Editor: Sandra Lemmon

Clathrin-dependent endocytosis is a major route for the cellular import of macromolecules and occurs at the interface between the cell and its surroundings. However, little is known about the influences of cell–substrate attachment in clathrin-coated vesicle formation. Using biochemical and imaging-based methods, we find that cell–substrate adhesion reduces the rate of endocytosis. Clathrin-coated pits (CCPs) in proximity to substrate contacts exhibit slower dynamics in comparison to CCPs found more distant from adhesions. Direct manipulation of the extracellular matrix (ECM) to modulate adhesion demonstrates that tight adhesion dramatically reduces clathrin-dependent endocytosis and extends the lifetimes of clathrin structures. This reduction is in part mediated by integrin-matrix engagement. In addition, we demonstrate that actin cytoskeletal dynamics are differentially required for efficient endocytosis, with a stronger requirement for actin polymerization in areas of adhesion. Together, these results reveal that cell–substrate adhesion regulates clathrin-dependent endocytosis and suggests that actin assembly facilitates vesicle formation at sites of adhesion.

INTRODUCTION

Clathrin-dependent endocytosis is a major pathway for the internalization of lipids and receptor-bound macromolecules into eukaryotic cells and is critical for many biological processes including nutrient uptake and cell signaling (Conner and Schmid, 2003). Clathrin-dependent endocytosis occurs in multiple steps and involves the assembly of structural proteins, including clathrin, onto the cytoplasmic face of the plasma membrane to form clathrin-coated pits (CCPs). CCPs serve to concentrate the macromolecules destined for internalization. These CCPs then invaginate and pinch off to form vesicles that are transported into the cell. This process reshapes the membrane that forms the interface between the cell and its extracellular environment. However, previous studies have primarily focused on the intracellular factors, such as cytosolic accessory proteins and lipids, that regulate vesicle formation. In contrast, physical connections with the external environment, including whether cell–substrate contact influences clathrin-mediated endocytosis, are poorly understood.

Most cells in solid tissues grow adherently. To perform basic cellular processes such as proliferation and differentiation, these cells must attach to and spread on the surrounding network of ECM. The integrin family of transmembrane receptors are the principle cell surface adhesion receptors that mediate cell–matrix adhesion (Hynes, 2002). Activated integrins cluster in macromolecular assemblies, including focal adhesions and focal contacts, where they attach to the underlying substrate and mediate mechanical and chemical signals into and out of the cell. Focal adhesions are also sites that link the extracellular matrix (ECM) to the filamentous actin cytoskeleton (reviewed in Naumanen *et al.*, 2008).

The role of actin cytoskeletal dynamics during clathrin-coated vesicle formation is not fully understood. Although clear genetic and biochemical evidence indicates that cortical actin dynamics are required for endocytosis in budding yeast (Engqvist-Goldstein *et al.*, 2001), the requirement for actin assembly and disassembly during clathrin-coated vesicle formation in animal cells remains under debate. Distinct requirements for actin assembly during clathrin-coated vesicle formation have been reported in different cell types (Schafer *et al.*, 1998; Fujimoto *et al.*, 2000; Blanpied *et al.*, 2002; Moskowitz *et al.*, 2003; Merrifield *et al.*, 2005; Yarar *et al.*, 2005; Boucrot *et al.*, 2006; Lee *et al.*, 2006), and have also been suggested to be differ on distinct surfaces of the same cell (Yarar *et al.*, 2005; Saffarian *et al.*, 2009).

Here, we sought to elucidate the influence of adhesion on clathrin-coated vesicle formation. Using physiological and more defined substrates, we report that adhesion negatively regulates clathrin-dependent endocytosis. Moreover, we demonstrate that vesicle formation has different requirements for actin assembly, depending on the context of cellular substrate adhesion.

MATERIALS AND METHODS

Cell Culture

BSC1 cells stably expressing clathrin light chain (CLC)-enhanced green fluorescent protein (EGFP) or σ2-EGFP (kindly provided by T. Kirchhausen, HMS, Cambridge, MA) were maintained as described (Ehrlich *et al.*, 2004). All plasmids were transfected with Lipofectamine 2000 (Invitrogen, Carlsbad,

This article was published online ahead of print in *MBoC in Press* (http://www.molbiolcell.org/cgi/doi/10.1091/mbc.E09–12–1044) on July 14, 2010.

Address correspondence to: Defne Yarar (yarar@wi.mit.edu).

Abbreviations used: CCP, clathrin-coated pit; TIR-FM, total internal reflection fluorescence microscopy; CLC-EGFP, clathrin light chain—enhanced green fluorescent protein fusion; IRM, interference reflection microscopy, BSA, bovine serum albumin.

CA) according to manufacturer's instructions and imaged 16–20 h after transfection.

Plasmids

mCherry-Paxillin was kindly provided by C. Waterman (NIH, Bethesda, MD) and dynamin1-mRFP by S. Schmid (TSRI; La Jolla, CA) (Soulet *et al.*, 2005).

Fluorescence Microscopy

Coverslips (no. 1.5, Corning, Corning, NY) or 35-mm uncoated MatTek dishes (Nunc, Waltham, MA) were precoated with poly-L-lysine (PLL; 1 mg/ml) for 1 h at 37°C, washed three times with dH_2O, dried completely, and then coated with either fibronectin (50 μg/ml, BD Biosciences, San Jose, CA), heat-denatured bovine serum albumin (BSA), or concanavalin A (conA) overnight at 4°C, and washed with phosphate-buffered saline (PBS). Coverslips were precoated with PLL to allow cells to lightly attach to BSA-coated coverslips; in the absence of PLL, cells did not adhere to BSA-coated coverslips. Cells, ($n = 1.2 \times 10^5$) were detached from near confluency using PBS + 5 mM EDTA, plated onto coverslips in serum-free medium (SFM; DMEM containing 10 mM HEPES, pH 7.4), and allowed to adhere for 1–3 h. To image cells on uncoated coverslips/MatTek dishes, $3–4 \times 10^4$ cells were seeded and incubated for ~48 h at 37°C. For inhibition of β1 integrin–mediated adhesion studies, anti-β1 integrin inhibitory antibody, AIIB2 (8 μg/ml; Developmental Studies Hybridoma Bank, Iowa City, IA) or control mouse antibody (8 μg/ml) was included when cells were seeded on fibronectin-coated coverslips in SFM. Alternatively, antibodies were included when cells were seeded on coverslips in Optimem (Invitrogen) and incubated for 48 h.

Cells were imaged in DMEM (no phenol red), 2.5% FCS, and 10 mM HEPES, pH 7.4. In experiments with inhibitory antibodies, cells were imaged in Optimem supplemented with antibodies. Images of mCherry/monomeric red fluorescent protein (mRFP)- or EGFP-fusion proteins were collected at 2–3-s intervals with an inverted microscope (TE2000U, Nikon, Garden City, NY) modified to allow for through-the-objective multispectral total internal reflection fluorescence microscopy (TIR-FM) using a 100×, 1.45 NA objective (Nikon). Exposure times of 50–200 and 500–600 ms were used for imaging EGFP- and mCherry/mRFP- fusion proteins, respectively. The wavelength and intensity of the 2 W multiline laser (Coherent, Santa Clara, CA) were controlled with an AOTF (488/568 lines). We used a evanescent field depth of ~200 nm. Fluorescence emission was controlled with a filter wheel device (Sutter Instruments, Novato, CA) containing narrow bandpass emission filters. Control of all electronic hardware and camera acquisition was achieved with MetaMorph software (Molecular Devices, West Chester, PA). Stage temperature and CO_2 levels were controlled with an environmental chamber (Solent Scientific, Segensworth, United Kingdom) maintained at 37°C. IRM images were acquired before and after time courses for subsequent analysis.

To visualize actin, cells were microinjected with X-rhodamine actin (0.5 mg/ml) and incubated for 3–7 h before imaging. Cells were then imaged as above, except that culture medium was supplemented with 1.0 U oxyrase per ml (Oxyrase, Mansfield, OH).

For indirect immunofluorescence, cells were plated onto coverslips and fixed with 4% paraformaldehyde for 25 min at room temperature. Cells were permeabilized in PBS containing 0.1% saponin and 2% BSA and incubated with rabbit anti-fibronectin (kindly provided by R. Hynes, MIT), monoclonal anti-paxillin antibodies (BD Biosciences, San Jose, CA), anti-β1 integrin antibodies (9EG7 clone that recognizes ligand bound β1, BD Biosciences), or Cy3-conjugated anti-rabbit/mouse/rat secondary antibodies (Jackson Laboratory , Bar Harbor, ME). Stained cells were mounted in Fluoromount G (Electron Microscopy Sciences, Hatfield, PA) imaged using an inverted Delta Vision epifluorescence microscope (Applied Precision, Issaquah, WA), and a Cool Snap HQ2 CCD (Photometrics, Tucson, AZ). For β1 integrin colocalization analyses in fibronectin-attached cells images were acquired by TIR-FM, and for β1 integrin colocalization analyses in cells plated on uncoated coverslips for 48 h images were acquired by scanning-confocal microscopy. For analysis, the average signal from the secondary antibody alone was subtracted from the β1 integrin image. Images were each separately contrast enhanced to optimize detection of β1 integrin foci, pseudocolored, and merged using Metamorph software. Diffraction-limited CCPs were chosen at random in the absence of the β1 integrin signal and then analyzed for colocalization with β1 integrin.

Image Analysis of Living Cells

CCPs were defined as diffraction-limited, individual structures that never split into multiple species. Clathrin-labeled structures that were larger than diffraction-limited CCPs were chosen as large clathrin assemblies. To avoid internal organelles, rapidly moving structures and structures lasting for less than eight consecutive frames were excluded from analysis. For analysis of clathrin dynamics near/far from sites of adhesion, clathrin structures within (≤20 pixels; 850 nm) and outside (>20 pixels) zones of adhesions, (identified in IRM or mCherry-paxillin images) were selected on predefined frames of the time-lapse movie. The duration from the first appearance to the frame before disappearance was used to determine CCP/clathrin-coated structure (CCS) lifetime.

To determine the fraction of CCPs that colocalize with dynamin-mRFP or x-rhodamine actin, images from time-lapse movies were pseudocolored red (for dynamin or actin) and green (for CLC) and merged. Green, diffraction-limited CCPs were first identified in the absence of the red channel. Then, with the red channel showing, the appearance of a red signal that was above the local background before the disappearance of the CCP was counted as a colocalization event.

For the perturbation of actin assembly, cells were perfused with latrunculin B (1 μM) after an initial 10-min time course and imaged for another 10 min with TIR-FM. Only lifetimes of CCPs before or after latrunculin B treatment that terminated with the colocalization of dynamin-mRFP were analyzed. Large clathrin structures were excluded from this analysis. An IRM or mCherry-paxillin image after the time course was used to determine regions close to and more distant from the coverslip. Surface density of clathrin structures was determined by averaging the number of CCPs in regions on two initial and final frames before or after latrunculin B treatment and expressed as the average number of clathrin structures per micrometer of surface area.

Biochemical Assays

Transferrin endocytosis assays were modified from (Smythe *et al.*, 1992; Carter *et al.*, 1993). Cells were detached, seeded onto fibronectin or BSA-coated coverslips, and allowed to adhere for 1 h as described above. The time course of internalization was initiated by adding serum-free medium containing biotin-conjugated transferrin (4 μg/ml). Internalization was stopped by placing coverslips on ice. Sequestration from avidin and processing of signal was performed as previously described (Smythe *et al.*, 1992; Carter *et al.*, 1993). The level of biotin-transferrin internalization was normalized to the amount of internalization for cells plated on BSA to account for day-to-day variation. Horseradish peroxidase (HRP) uptake assays were performed as previously reported (Schlunck *et al.*, 2004), with the exception that cells were plated on fibronectin or BSA-coated coverslips, as described above.

To measure adhesion levels, cells were plated on coated coverslips as described above and allowed to adhere for 1–2 h. Coverslips were then washed three times with PBS by trituration and resuspended in phosphatase substrate (Sigma, St. Louis, MO) in lysis buffer (0.4% Triton X-100, 50 mM sodium citrate, pH 6.5). Remaining cells were quantified by OD 405 nm and expressed as the percent of total cells plated.

Whiskers of box plots are presented from 5 to 95 percentiles. Mean and outliers are marked as open circles and asterisks, respectively. Statistical analyses were performed with Minitab statistical software (Minitab, State College, PA) (www.minitab.com). Experiments with more than two populations were analyzes using ANOVA combined with Tukey multiple comparison test.

RESULTS

To study the influence of adhesion on clathrin-dependent endocytosis, we used BSC1 epithelial cells stably expressing EGFP-tagged CLC (Ehrlich *et al.*, 2004). These flat cells are well suited to both microscopic- and biochemical-based analyses. We first determined if the rate of CCP dynamics differed in distinctly adherent membrane regions within the same cell. To this end, we incubated cells on coverslips for ~48 h in the presence of a complex composition of ECM derived from the serum-containing culture medium and ECM molecules secreted by the cells. We imaged CLC-EGFP dynamics on the ventral plasma membrane of cells using time-lapse *t*otal *i*nternal *r*eflection *f*luorescence *m*icroscopy (TIR-FM) and visualized the pattern of cell–substrate adhesion using *i*nterference *r*eflection fluorescence *m*icroscopy (IRM), a method in which regions of the plasma membrane closer to the coverslip appear dark (Curtis, 1964; Figure 1A). In contrast to the uniform, diffraction-limited clathrin structures observed under shorter incubation periods (Ehrlich *et al.*, 2004; Loerke *et al.*, 2009), cells allowed to attach to coverslips for two days contained a heterogeneous population of CCSs, including both diffraction-limited CCPs and larger clathrin assemblies (Figure 1). Interestingly, the majority of the large clathrin assemblies overlapped with or were immediately adjacent to (within 850 nm) regions of the cell close to substrate attachment sites (Figure 1, A and B). Similar structures have been detected in a variety of cell types (Rappoport and Simon, 2003; Keyel *et al.*, 2004; Yarar *et al.*, 2005). As a complimentary approach, we transiently expressed mCherry-paxillin to mark focal adhesions and quantified the fraction of large clathrin assemblies and CCPs

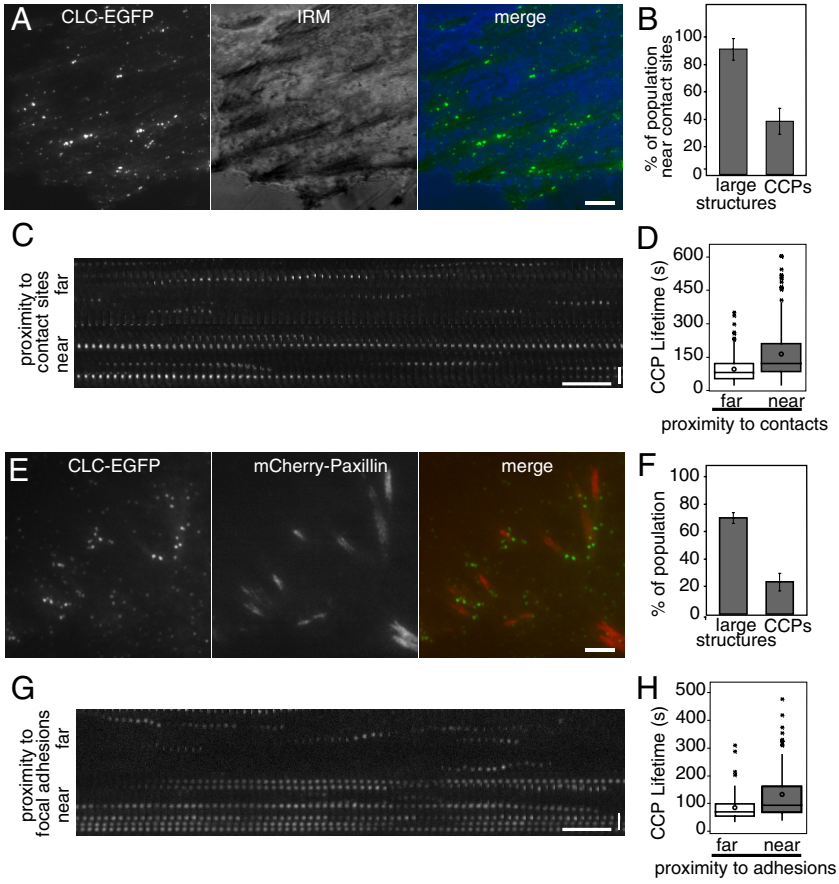

Figure 1. Clathrin dynamics are distinct at sites of substrate adhesion. (A) CLC-EGFP imaged by TIR-FM (left, green in merge) and the ventral cell surface imaged by IRM (center, blue in merge) show that large clathrin structures overlap with substrate contact sites. BSC1 cells were plated in serum-containing medium for 48 h. (B) Bar graph showing mean percentage (±SEM) of large clathrin structures or CCPs adjacent to/overlapping with substrate contact regions, as determined by IRM. n ≥ 399, 21 cells (each clathrin class). (C) Kymograph of representative clathrin structures near and far from substrate contact sites. (D) Box plots showing the distribution of lifetimes of diffraction-limited CCPs, based on their relative proximity to sites of adhesion. n ≥ 283 CCPs, 15 cells/category. Populations were significantly different; $p < 0.05$, Student's t test. See Supplemental Movie 1. (E) TIR-FM images of CLC-EGFP (left, green in merge) and mCherry-paxillin (center, red in merge). (F) Bar graph showing the mean percentage (±SEM) of large clathrin structures or CCPs adjacent to/overlapping with mCherry-paxillin labeled focal adhesions. n ≥ 404, 20 cells/each clathrin classification. (G) Kymograph of representative clathrin structures based on their relative proximity to mCherry-paxillin-labeled focal adhesions. (H) Box plots showing the distribution of lifetimes of diffraction-limited CCPs based on their relative proximity to mCherry-paxillin–labeled focal adhesions. n ≥100 CCPs, four cells/category. Populations were significantly different; $p < 0.001$, Student's t test. See Supplemental Movie 2. Scale bars in cells, (A and E) 5 μm. Scale bars in kymographs, time = 1 min and distance = 2 μm.

that could be observed overlapping with or lying adjacent (within 850 nm) to focal adhesions. Similarly, the majority of large clathrin structures were found in these areas (Figure 1, E and F). These data suggest that the local environment near sites of cell–substrate contact may influence the behavior of clathrin-coated structures.

Traditional, diffraction-limited CCPs (<250 nm in size) are the major carriers for endocytic cargo into cells (Conner and Schmid, 2003) and have recently been suggested to fulfill the majority of the endocytic capacity of the cell (Saffarian *et al.*, 2009). As a first approach to determine if there is a connection between clathrin-dependent endocytosis and substrate adhesion, we measured the lifetimes of diffraction-limited CCPs in regions of the plasma membrane in relation to substrate-contact sites, as determined by IRM. Manual analysis of CCP lifetimes (defined as the moment of the first appearance to the last time point before disappearance) revealed that CCPs closely apposed to the coverslip persisted for 1.7 times longer (164 ± 7 s; Student's t test; $p < 0.001$) than CCPs in unattached membrane zones (96 ± 3 s; Figure 1, C and D; Supplemental Movie 1). Lifetimes of randomly selected CCSs (including both diffraction-limited CCPs and larger CCSs) were also significantly longer ($p < 0.001$, Student's t test) in membrane regions close to the substrate than regions farther from the substrate (Supplementary Figure S1). Similarly, the analysis of CCP lifetimes in relation to mCherry-paxillin–labeled focal adhesions revealed an increase in CCP lifetimes near adhesions (132 ± 9; $p < 0.001$) in comparison to CCPs more distant from focal adhesions (85 ± 5 s; Figure 1, G and H; Supplemental Movie 2). CCP lifetimes were also found to be significantly longer at sites of adhesion using spinning-disk confocal imaging, which samples a thicker optical section, excluding the possibility that CCP lifetimes as determined by TIR-FM resulted from a longer duration in the evanescent field (unpublished data). Taken together, these data demonstrate a spatial heterogeneity of CCP lifetimes in cells that correlates with the nature of the underlying substrate attachment, with slowly internalizing CCPs localizing near sites of substrate adhesion.

Adhesion to Fibronectin Slows the Rate of Transferrin Endocytosis

To test directly whether cell–substrate adhesion influences clathrin-mediated endocytosis, we next assessed the effects of tight cellular adhesion under more defined adhesion conditions. To this end, we coated coverslips with saturating levels of fibronectin (50 μg/ml; Supplemental Figure S2A), an ECM molecule secreted by BSC1 cells (Supplemental Figure S2, B and C). As a control, we used coverslips coated with heat denatured BSA, a substrate previously used to generate weak adhesion conditions (Gupton and Waterman-Storer, 2006; Figure 2A). To minimize the confounding effects that may arise from modification of the underlying substrate by endocytosis or exchange with proteins in the culture medium, cells were only allowed to attach to the coated coverslips for a short interval (1–3 h) in serum-free medium. Cells adhered to fibronectin were spread, often pancake-shaped, and formed mature focal adhesions (Figure 2, B and C). In contrast, most cells plated on BSA-coated coverslips did not spread well, exhibited thick, phase-dense ruffles, and sometimes formed smaller focal contacts (Figure 2, B and C), indicative of their weak adhesion state.

Using these two distinct adhesion conditions, we analyzed the internalization of transferrin, a ligand for constitutive cath-

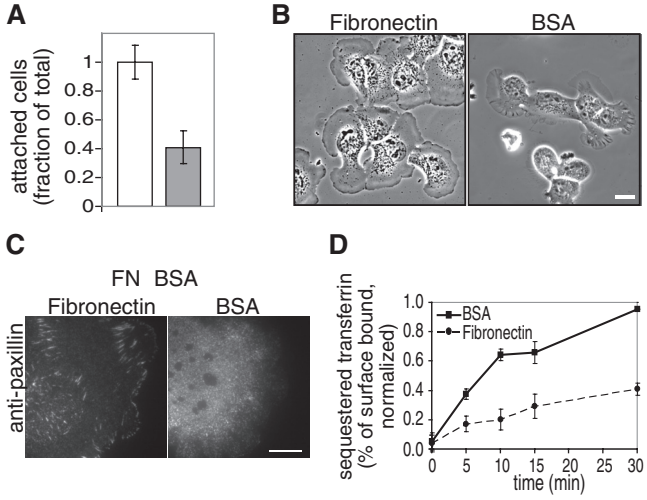

Figure 2. Tightly adhered cells exhibit a reduced rate of endocytosis in comparison to weakly adhered cells. Defined conditions were developed for tight and weak adhesion, shown in (A) an adhesion assay and (B) phase-contrast images of cells plated on fibronectin- and heat-denatured BSA-coated coverslips. Cells are tightly adhered to fibronectin- (□) but poorly attached to BSA (▨)-coated coverslips. Data are shown as mean ± SD, n = three independent experiments. Cells were plated on coated coverslips in serum-free medium for 1- 3 h. (C) Anti-paxillin immunofluorescence TIR-FM images of cells plated on fibronectin- (left) and BSA (right)-coated coverslips are presented, showing the morphology and size of focal adhesions/contacts. Scale bars, 10 μm. (D) Tight adhesion reduces clathrin-dependent endocytosis of transferrin. Time courses of biotin-conjugated transferrin sequestered from avidin in cells plated on fibronectin- (●, dashed line) and BSA (■, solid line)-coated coverslips as in B are shown, demonstrating that clathrin-mediated endocytosis is significantly slowed in cells plated on fibronectin-coated coverslips in comparison to cells plated on BSA-coated coverslips ($p < 0.05$, Student's t test). Results are shown as a percent of the total surface-associated transferrin. Data are normalized to maximum endocytosis levels and shown as mean ± SD, n = four duplicate experiments.

rin-mediated endocytosis, biochemically (Smythe *et al.*, 1992; Carter *et al.*, 1993). Cells adherent to fibronectin-coated coverslips internalized transferrin at a significantly slower rate than those adherent to BSA-coated coverslips (60% reduction in uptake from 0 to 5 min, $p < 0.05$, Student's t test; Figure 2D). Moreover, transferrin receptor surface levels were 1.8 ± 0.3 (mean ± SD) fold higher in cells adherent to fibronectin than in cells adherent to BSA, consistent with the reduction in rates of endocytosis. Cells attached to BSA-coated coverslips exhibited phase-dense ruffles (Figure 2B and data not shown), structures that have been correlated with fluid-phase internalization (Conner and Schmid, 2003). Thus, we also quantitatively measured the fluid-phase uptake of HRP. In contrast to the difference observed in transferrin internalization, we did not detect a difference in HRP internalization in cells plated on fibronectin compared with that of cells plated on BSA-coated coverslips (Supplemental Figure S3). This indicates that the difference in the rate of transferrin uptake reflects a reduction in clathrin-mediated endocytosis upon adhesion and not a change in bulk fluid-phase internalization.

Adhesion to Fibronectin Slows CCP Dynamics

Our biochemical analysis of endocytosis under defined substrate conditions demonstrates that a quantitative change in endocytosis occurs upon substrate adhesion in a population of cells. To test the effects of adhesion on individual cells, we imaged CLC-EGFP dynamics on the ventral plasma membrane of cells plated under the same conditions (on fibronectin- or BSA-coated coverslips for 1–3 h) using time-lapse TIR-FM. Analysis of the lifetimes of diffraction-limited CCPs demonstrated that CCPs bound to fibronectin persisted longer (440 ± 10 s) than CCPs in cells under less adhesion (BSA; 98 ± 5 s; Figure 3, A and B, $p < 0.05$, ANOVA; Supplemental Movie 3). Although these values indicate a significant difference in lifetimes, the analysis may underestimate CCP lifetimes in cells attached to fibronectin-coated coverslips because 25% of the CCPs persisted for the full 10 min of the time course (Figure 3B). One possible explanation for the shorter-lived CCPs in cells under low-adhesion conditions is that membrane fluctuations move CCPs prematurely out of the illuminated optical section and abbreviate the apparent CCP lifetime. Because dynamin GTPase is essential for clathrin-dependent endocytosis (van der Bliek and Meyerowitz, 1991; Damke *et al.*, 1994) and exhibits a single peak of recruitment to CCPs immediately before vesicle formation (Merrifield *et al.*, 2002; Rappoport and Simon, 2003; Ehrlich *et al.*, 2004), we monitored dynamin recruitment to exclude nonproductive endocytic events. We predicted that if the disappearance of CLC-EGFP does not correlate with vesicle formation, a peak of dynamin-mRFP recruitment at the CCP would not coincide with internalization. However, a peak of dynamin-mRFP transiently localized with the majority of the diffraction-limited clathrin structures (80 ± 3%; n = 6 cells, 350 CCPs) before their disappearance in cells on BSA-coated coverslips, confirming that the loss of the CLC-EGFP signal was not due to movement out of the illuminated optical section (Figure 3C, Supplemental Movie 4).

We next determined if the proximity of diffraction-limited CCPs to focal adhesions in cells attached to coverslips uniformly coated with fibronectin influenced CCP dynamics. Interestingly, we detected a small, yet significantly longer average lifetime for CCPs found close to mCherry-paxillin labeled adhesions (424 ± 19 s) in comparison to those far from adhesions (350 ± 15 s) in the majority of fibronectin-adherent cells analyzed (Student's t test, three of four cells, $p < 0.05$; Figure 3D). In addition, the lifetimes of the CCPs far from the focal adhesions in fibronectin-adherent cells were significantly longer than CCP lifetimes in cells plated on BSA (98 ± 5 s, $p < 0.05$, ANOVA). This may reflect the difference in the size and nature of the adhesions or the underlying cytoskeleton that forms in these different conditions and is consistent with the idea that a uniform coating of high levels of fibronectin-mediated adhesion has both local and global effects on CCP dynamics.

Other Modes of Adhesion May Also Regulate CCP Dynamics

To determine if the adhesion-mediated reduction in CCS dynamics is specific to fibronectin-mediated adhesion or if adhesion to another unrelated substrate is sufficient to reduce CCP dynamics, we plated cells on coverslips coated with the plant lectin conA. ConA binds to the glycoproteins residing on the cell surface and does not induce signaling. Analysis of diffraction-limited CCP dynamics from time-lapse TIR-FM movies revealed that nearly all CCP dynamics were lost in cells plated on conA, with an average lifetime of 596 ± 2 s (Figure 3, E and F). We are underestimating the lifetimes of these CCPs, however, as most of the CCPs persisted for the full length of the 10-min time course. This indicates that an adhesion-mediated reduction in CCP dy-

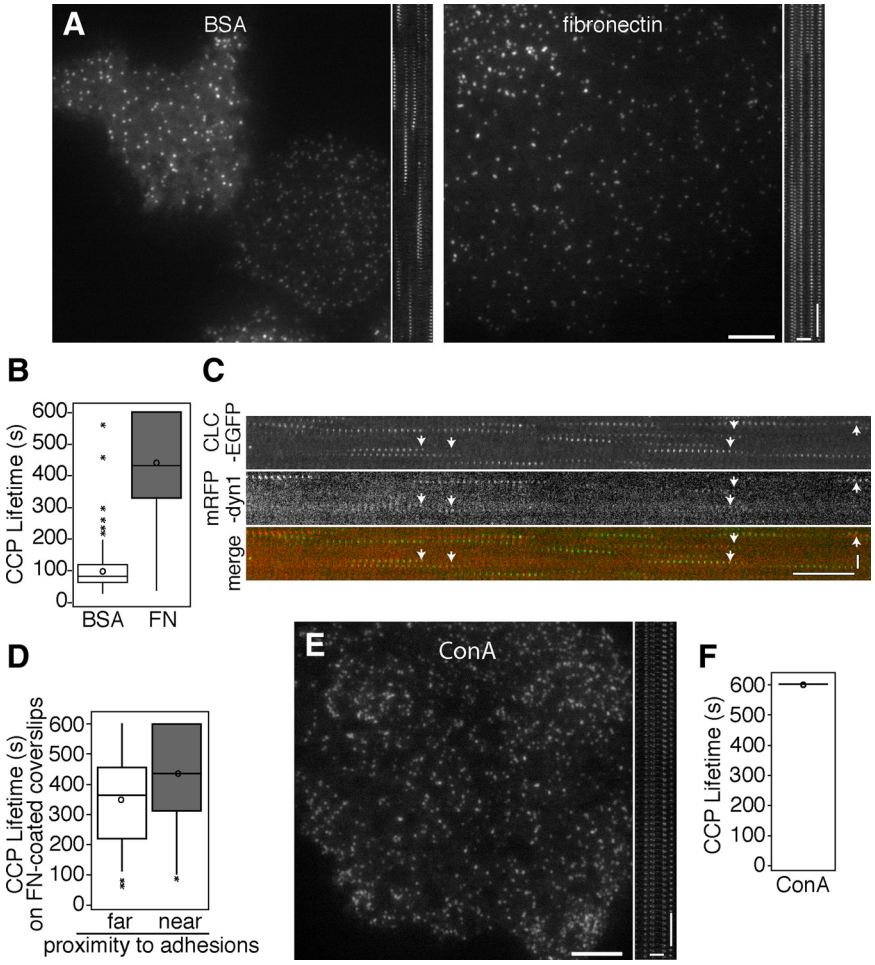

Figure 3. Clathrin-coated structures have increased lifetimes in tightly adhered cells. (A) TIR-FM images and (B) box plots showing CCP lifetime distributions in cells plated on fibronectin- and BSA-coated coverslips for 1–3 h in serum-free medium. Corresponding kymographs made from rectangular regions are shown to right of the images in A. $n \geq 200$, five cells each condition. Populations of lifetimes were significantly different, $p < 0.05$, ANOVA. See Supplemental Movie 3. (C) TIR-FM kymographs of CLC-EGFP (top, green in merge) and dynamin-mRFP (middle, red in merge) from cells plated on BSA-coated coverslips are presented, showing CCPs recruit dynamin late in vesicle formation. See Supplemental Movie 4. (D) Box plots showing the distribution of lifetimes of CCPs based on their relative proximity to mCherry-paxillin-labeled focal adhesions in cells plated on fibronectin-coated coverslips for 1–3 h in serum-free medium. $n \geq 145$, four cells. CCP lifetimes near and far from adhesions were significantly different in 3–4 cells, $p < 0.05$, Student's *t* test. (E) TIR-FM image and (F) box plots showing CCS lifetime distributions of cells plated on conA- coated coverslips. Cells were incubated for 1–3 h in serum-free medium. Corresponding kymograph made from rectangular region is shown to the right of image. $n \geq 125$, four cells each condition. See Supplemental Movie 5. Scale bars in cells, 5 μm. Scale bars in kymographs, time = 1 min and distance = 2 μm.

namics is not fibronectin specific. Although the mechanisms that reduce CCP dynamics in cells plated on conA and fibronectin may be distinct, these observations underscore the importance of cell–substrate adhesion on clathrin-dependent endocytosis.

A Subset of CCPs Colocalize with Active β1 Integrin

Cells attach to the ECM through integrins, heterodimeric transmembrane proteins at the cell surface (Hynes, 2002). In combination with a number of different α subunits, β1 integrin has been shown to be important for binding to fibronectin. BSC1 cells express β1 integrin, which localizes on the cell surface in punctate and linear patterns, likely corresponding to focal contacts and adhesions, respectively (Figure 4). One possible mechanism to explain how tight adhesion reduces clathrin-mediated endocytosis is that clathrin structures at sites of adhesion are loaded with integrins that are directly attached to the ECM and consequently are retained at the cell surface. To test this, we measured the colocalization of diffraction-limited CCPs with β1 integrin bound to the ECM in relation to focal adhesions in cells grown in serum for 48 h. We used indirect immunofluorescence with an antibody that specifically recognizes a ligand-bound conformation of β1 integrin (9EG7; Lenter *et al.*, 1993) and identified focal adhesions with an anti-paxillin antibody. Analysis of images taken with confocal microscopy indicated a significant increase in the fraction of CCPs overlapping with ECM-bound β1 integrin at sites of adhesion (55 ± 3; $p < 0.001$, Student's *t* test) in comparison to CCPs away from adhesions (27 ± 4; Figure 4). This suggests that physical association CCPs with the ECM through β1 integrin may contribute to the inhibition of vesicle formation. Consistent with this, a greater fraction of CCPs overlapped with ligand-bound β1 integrin in cells plated on fibronectin-coated coverslips ($19 \pm 6\%$) in comparison to CCPs in cells plated on BSA-coated coverslips and imaged with TIR-FM ($11 \pm 1\%$; $p < 0.001$, Student's *t* test). Although these data suggest that β1 integrin molecules directly attached to the ECM reduce clathrin dynamics, they do not account for the prolonged lifetime measured for >75% of the CCPs in fibronectin-adherent cells in comparison to CCPs found in cells attached to BSA-coated coverslips. Thus, the adhesion-mediated inhibition of clathrin-coated vesicle formation may be partially explained by a direct physical attachment of clathrin structures to the underlying matrix through β1 integrin.

Reduction in CCP Dynamics Is Mediated by β1 Integrin

Because a higher fraction of CCPs under conditions of high adhesion colocalized with ligand-bound β1 integrin, we investigated the contribution of β1 integrin function to vesicle formation. We first tested the effect of a function-blocking β1 integrin antibody (AIIB2; 8 μg/ml) on CCPs dynamics in cells plated on coverslips in serum-containing medium for 48 h. However, we did not observe a difference in cell morphology or CCP dynamics (data not shown). Because serum contains a combination of ECM molecules (e.g., vi-

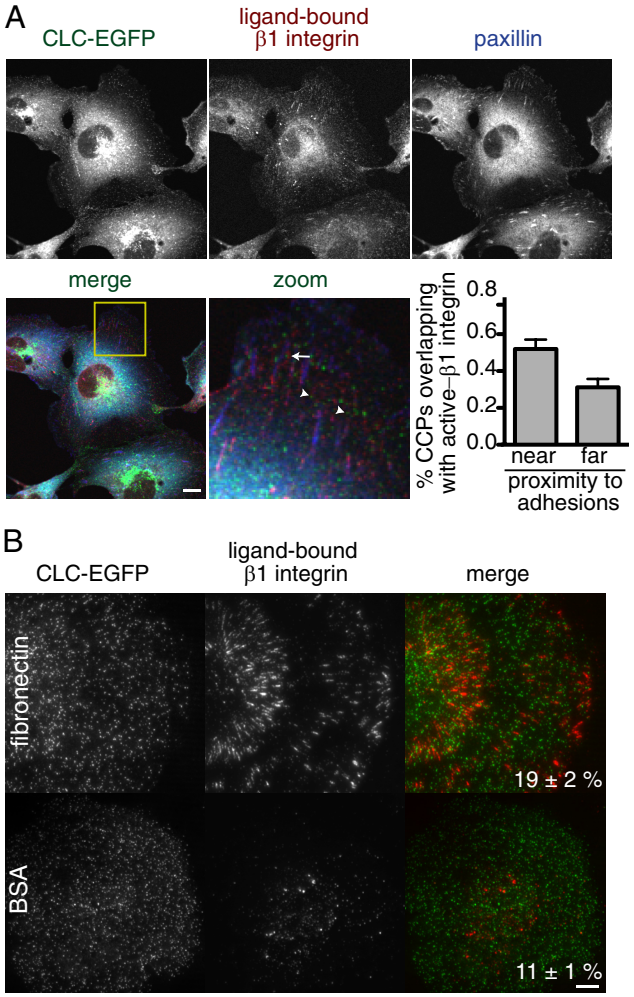

Figure 4. Ligand-bound β1 integrin colocalizes with CCPs at focal adhesions. (A) Indirect immunofluorescence images (imaged by scanning confocal microscopy) of ECM-bound β1 integrin (top center panel, red in merge) and paxillin (top right panel, blue in merge) in BSC1 CLC-EGFP expressing cells plated for 48 h on coverslips in serum-containing medium. CLC-EGFP (top right panel, green in the merge) is also shown. Examples of CCPs overlapping with ECM-bound β1 integrin near (arrow) and far from (arrowheads) focal adhesions are indicated. Bar graph showing the percent (±SEM) of CCPs that overlap with the ECM-bound β1 integrin near and far from focal adhesions is shown (n ≥ 780 CCPs, 14 cells). The fraction of CCPs overlapping with β1 integrin was significantly greater near focal adhesions ($p < 0.001$, Student's *t* test). Magnification of yellow-boxed area in merge also shown. (B) Indirect immunofluorescence images (imaged by TIR-FM) of ECM-bound β1 integrin (middle panels, red in merge) in BSC1 CLC-EGFP (left panels, green in merge) cells plated on fibronectin- (top) and BSA (bottom)-coated coverslips. The average percent (±SEM) of CCPs that overlap with the ECM-bound β1 integrin is shown (n ≥ 1100 CCPs, 20 cells/condition) and is significantly different ($p < 0.001$, Student's *t* test). Scale bars, 5 μm.

tronectin and fibronectin), we tested the effect of β1 integrin inhibition on CCPs dynamics in cells allowed to attach to coverslips in serum-free medium for an extended period (48 h), allowing the cells to attach to matrix that they themselves secreted. The lifetimes of diffraction-limited CCPs in the vicinity of adhesions revealed that CCPs in anti-β1 integrin antibody (AIIB2; 8 μg/ml)-treated cells were significantly shorter lived (129 ± 5 s, $p < 0.01$, Student's *t* test) than CCPs in control antibody treated cells (200 ± 8 s; Figure 5, A and B, Supplemental Movie 6). This demonstrates that the β1 integrin-ECM attachment contributes to the adhesion-mediated inhibition of CCP dynamics.

We next determined whether β1 integrin mediates the reduction in CCP lifetime in cells attached to uniformly coated coverslips by treating cells with anti-β1 integrin inhibitory (AIIB2; 8 μg/ml) or a control antibody during adhesion with short incubation times. In contrast to cells incubated with control antibodies, cells treated with the β1 integrin inhibitory antibody formed phase-dense, ruffled lamellipodia, consistent with the reduction of adhesion (data not shown). The average lifetime of diffraction-limited CCPs in anti-β1 integrin antibody-treated cells plated on fibronectin was significantly shorter (185 ± 9 s) than the lifetime of CCPs in control antibody treated cells (419 ± 13 s; Figure 5, C and D, $p < 0.05$, Student's *t* test; Supplemental Movie 7), demonstrating that the reduction in endocytosis in fibronectin-attached cells is β1 integrin dependent. The extent of rescue of CCP lifetimes was incomplete, however, when compared with CCPs lifetimes in cells plated on BSA-coated coverslips (185 vs. 98 s). This suggests that either the antibody does not completely inhibit β1 integrin function, or other modes of adhesion also contribute to the reduction of clathrin-mediated endocytosis in cells adherent to uniformly coated fibronectin. Taken together, these data demonstrate that β1 integrin-mediated adhesion negatively influences CCP dynamics.

Actin Dynamics Are Required for Efficient Endocytosis

Because the lifetimes of CCPs can be differentiated by their proximity to the underlying substrate, we sought to determine if there are distinct molecular requirements for vesicle formation under different adhesion conditions. We hypothesized that attachment of a CCP to the matrix, for example through β1 integrin, would be expected to resist membrane deformation. Because actin polymerization is sufficient to drive the motility of a load (Loisel *et al.*, 1999), we sought to determine if endocytosis at sites of cell–substrate adhesion preferentially requires actin polymerization. However, whereas the role of actin assembly and disassembly dynamics in endocytosis has been demonstrated in some cells (Blanpied *et al.*, 2002; Moskowitz *et al.*, 2003; Merrifield *et al.*, 2005; Yarar *et al.*, 2005; Lee *et al.*, 2006), the role of actin in other cell types, including the BSC1 cells used in this study (Fujimoto *et al.*, 2000; Boucrot *et al.*, 2006; Saffarian *et al.*, 2009), remains under debate. As a first step, we demonstrated that diffraction-limited CCPs in BSC1 cells recruit actin during vesicle formation in cells microinjected with fluorescently labeled actin (Figure 6A, Supplemental Movie 8), similar to CCPs in a variety of other cell types (Merrifield *et al.*, 2002; Benesch *et al.*, 2005; Yarar *et al.*, 2005). A similar fraction of diffraction-limited CCPs in regions both near (54 ± 2%, n = 5 cells, 206 CCPs) and far (53 ± 3%, n = 5 cells, 180 CCPs) from sites of substrate adhesion as determined by IRM colocalized with actin before their disappearance. To determine if actin assembly plays a role in clathrin-coated vesicle formation in BSC1 cells, we acutely treated cells plated on coverslips for 48 h in the presence of serum-containing medium with a low concentration of latrunculin B (1 μM), a pharmacological agent that sequesters actin monomers and inhibits actin assembly (Spector *et al.*, 1989). After an initial time course, cells were perfused with 1 μM latrunculin B. Under these conditions focal adhesions persisted and cells did not detach dramatically from the substrate (Figure 6). However, the motile behaviors of the CCPs changed upon inhibition of actin assembly; many CCPs in

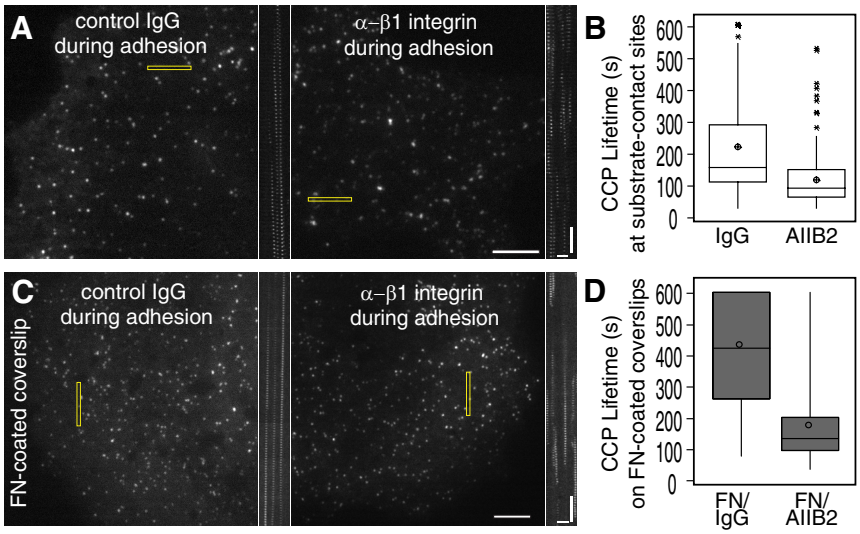

Figure 5. β1 integrin–dependent adhesion reduces CCP dynamics. (A and B); TIR-FM images (A) and box plots (B) showing lifetime distributions of CCPs at sites closest to the coverslip in cells plated on "uncoated" coverslips in the presence of either control IgG (left) or inhibitory β1 integrin antibody (AIIB2; right). Cells were incubated for 48 h on the coverslip in serum-free medium. Corresponding kymographs made from the rectangular regions are shown to the right of images. n ≥ 120 CCPs, six cells/condition. Populations of lifetimes were significantly different, $p < 0.01$, ANOVA. See Supplemental Movie 6. (C) TIR-FM images and (D) box plots showing lifetime distributions of CCPs in cells plated on fibronectin (FN)-coated coverslips and incubated with either control IgG (left) or inhibitory β1 integrin antibody (AIIB2; right) during adhesion. Cells were incubated for 1–3 h in serum-free medium. Corresponding kymographs made from the rectangular regions are shown to right of images. n = 165 CCPs, five cells/condition. Populations of lifetimes were significantly different, $p < 0.05$, ANOVA. See Supplemental Movie 7. Scale bars in cells, 5 μm. Scale bars in kymographs, 1 min and 2 μm.

areas without adhesion increased in their rate of lateral movement (Supplemental Movie 9, data not shown), as previously observed (Gaidarov *et al.*, 1999; Boucrot *et al.*, 2006).

The increase in CCP movement upon disassembly of the actin cytoskeleton has been shown to correlate between multiple CCPs within a local area (Boucrot *et al.*, 2006), suggesting that large regions of the plasma membrane may become motile. Therefore, we measured lifetimes of diffraction-limited CCPs that transiently recruit dynamin-mRFP before their disappearance, to exclude events in which the loss of the CLC-EGFP signal resulted from fluctuations of the membrane and movement out of the illuminated optical section. Indeed, we observed a reduction in the proportion of diffraction-limited CCPs that colocalized with dynamin before their disappearance after latrunculin B treatment at sites far from the substrate (as determined by IRM; 80 ± 3% before vs. 56 ± 7% after latrunculin B treatment, $p < 0.05$; n = 4 cells, n ≥ 135 CCPs). This difference was not apparent for CCPs in membrane regions localized close to the underlying substrate (82 ± 2% before vs. 78 ± 3% after latrunculin B treatment, $p = 0.4$; n = 4 cells, n ≥ 135 CCPs). Strikingly, we found that disassembly of the actin cytoskeleton differentially affected CCP lifetimes, depending on the nature of the underlying cell–substrate contact. CCP lifetimes in both adherent and nonadherent regions of the membrane, as determined by IRM or mCherry-paxillin localization, were increased upon latrunculin B treatment, indicating that actin plays a role in endocytosis in BSC1 cells in both of these adhesive conditions (Figure 6, B and C, data not shown). However, CCP endocytosis in adherent regions of the membrane was more severely inhibited [130 ± 60% increase in lifetime (mean ± SD), n ≥ 150 CCPs, six cells] than in nonadherent regions (65 ± 37% increase in lifetime, n ≥ 150 CCPs, six cells; ANOVA, $p < 0.05$; Figure 6C, Supplemental Movie 9). Consistent with the severe inhibition in the rate of endocytosis, CCP density at sites of substrate contact was increased after disruption of actin dynamics (Figure 6D, $p < 0.01$, Student's *t* test). In contrast, CCP density did not significantly change in areas far from the substrate ($p < 0.4$, Student's *t* test). We also tested the effect of latrunculin B treatment in cells plated on fibronectin-coated coverslips and found that CCP lifetimes were increased by 1.7-fold (data not shown). The parallel experiment in cells plated on low adhesive conditions was technically challenging because upon treatment with latrunculin B, many of these cells detached from the coverslip, precluding their analysis (data not shown). Taken together, these data indicate that actin assembly plays a role in efficient coated vesicle formation in regions of the cell with and without substrate contact, but is preferentially required for clathrin-coated vesicle formation in regions of adhesion.

DISCUSSION

Clathrin-dependent endocytosis occurs on the plasma membrane, the site of cell–substrate adhesion. Here, we used quantitative fluorescence microscopy, biochemistry, and molecular perturbations to demonstrate that substrate adhesion negatively influences clathrin-coated vesicle formation and generates spatial heterogeneity of CCP lifetimes on the cell surface. Furthermore, we find that the reduction of coated vesicle formation in cells adherent to the ECM molecule fibronectin is mediated in part by β1 integrin and that clathrin-dependent endocytosis at sites of adhesion is facilitated by a dynamic actin cytoskeleton.

Although previous studies on endocytosis have primarily focused on tissue culture cells grown in vitro, our discovery that adhesion influences endocytosis has important implications for the functions of cells that normally grow in the context of multicellular tissues surrounded by ECM. In addition to our demonstration that clathrin-dependent endocytosis is affected by interactions with the substrate, adhesion may more generally affect endocytosis. Indeed, substrate adhesion has been found to negatively regulate the uptake of the AMPA receptor through clathrin-dependent endocytosis and the internalization of caveolae (del Pozo *et al.*, 2005; Cingolani *et al.*, 2008). In addition, the density and number of clathrin assemblies observed on macrophages was reported to be greater on the adherent surface than on the free surface (Aggeler and Werb, 1982). Although many factors are involved in CCP formation and internalization, these data may be explained in part by an adhesion-mediated reduction in the kinetics of internalization. Together,

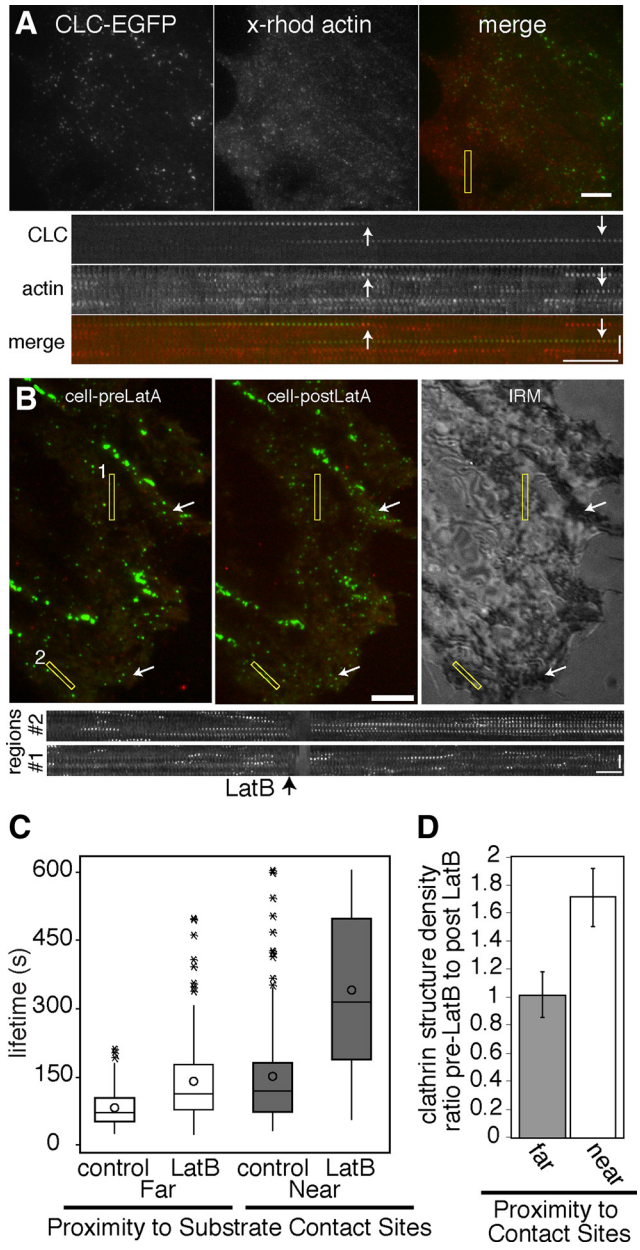

Figure 6. Actin cytoskeletal assembly is preferentially required for endocytosis at sites of substrate contact. (A) TIR-FM images and kymographs of CLC-EGFP and x-rhodamine actin, showing that actin is recruited to CCPs late during vesicle formation. Cell was plated in serum-containing medium for 48 h. See Supplemental Movie 8. (B) TIR-FM images of CLC-EGFP and dynamin-mRFP and corresponding IRM image showing pattern of adhesion. (C) Box plots showing the lifetime distributions of CCPs that transiently recruit dynamin. Cells plated on uncoated coverslips for 48 h in serum-containing medium were perfused with 1 μM latrunculin B after a 10-min time course. n = 150 CCP/adherent condition per five cells. Significant difference between populations (*$p < 0.05$, ANOVA). Corresponding kymographs generated from yellow rectangular regions (1 = near contact site; 2 = far from contact site) are shown. (D) Bar graph (mean ± SD) showing the ratio of CCP density before latrunculin B to after latrunculin B treatment in regions near to and far from the substrate (as determined by IRM) is significantly different ($p < 0.01$, Student's t test). Arrows in C. exemplify regions with increased CCP density after latrunculin B treatment. See Supplemental Movie 9. Scale bars in cells, 5 μm. Scale bars in kymographs, time = 1 min and distance = 2 μm.

these findings support a general role for adhesion in affecting multiple routes of endocytosis.

Mechanism of Adhesion-mediated Reduction in CCP Dynamics

There are two primary, nonmutually exclusive mechanisms by which substrate adhesion inhibits the rate of clathrin-dependent endocytosis. First, the inhibition of clathrin-dependent endocytosis may occur through a direct linkage of a CCP constituent with the underlying substrate that physically impedes internalization. Second, this inhibition may occur through an indirect, signaling-based route that functions through the modification of the endocytic machinery or the cell cortex.

In support of the idea that adhesion directly inhibits endocytosis, we found that a greater fraction of clathrin structures near focal adhesions overlapped with ECM-bound β1 integrin than clathrin structures more distant from focal adhesions. In addition, more CCPs in cells adherent to fibronectin-coated coverslips colocalized with ECM-bound β1 integrin than CCPs in cells adherent to BSA-coated coverslips. An interaction of CCPs with the underlying substrate was suggested previously by Maupin and Pollard (1983), who observed structures by EM that resembled a combination of flat and curved CCPs and clathrin-coated vesicles. These structures closely apposed the underlying substrate, especially in proximity to focal contacts. Also consistent with the notion that physical linkage to the underlying substrate restrains the CCP at the cell surface, we found that adhesion to conA-coated coverslips dramatically inhibits CCP dynamics.

In addition, to β1-integrin–mediated adhesion, our results also suggest that other methods of physical attachment to the underlying substrate may contribute to the reduction in CCP dynamics. First, although more CCPs colocalize with ECM-bound β1 integrin in cells grown on fibronectin- than BSA-coated coverslips, the majority of CCPs did not colocalize with active β1 integrin. However, ~75% of the CCPs in fibronectin-adherent cells exhibited longer lifetimes than all of the CCPs in cells plated on BSA-coated coverslips. Therefore, β1 integrin loading of CCPs cannot account for the reduction in the lifetimes of all of the CCPs under conditions of tight adhesion. This trend, although less dramatic, was also true in cells grown on coverslips with nonuniform substrates. However, because the analysis of fixed cells only provides information on a single time point in the life of a CCP and the interactions of β1 integrin with ECM are transient, we may be underestimating the fraction of CCPs that are filled with ECM-bound β1 integrin. Nevertheless, we observed only a partial rescue of adhesion-mediated inhibition of endocytosis upon perturbation of β1 integrin function, suggesting that other modes of substrate attachment to the matrix, including other integrins, may also influence CCP dynamics. Hence, there may be other ECM-associated integrins within CCPs or other nonintegrin modes of adhesions that influence CCP dynamics.

Although physical adhesion to the ECM may directly resist endocytosis, adhesion may influence clathrin-dependent endocytosis indirectly by converting mechanical information into chemical signals. A signal-based mechanism that reduces the rate of endocytosis would be expected to influence CCP dynamics in membrane regions distant from sites of adhesion. Consistent with this notion, it has been suggested recently that adhesion may have a global effect on CCP dynamics (Liu *et al.*, 2009). Indeed, our biochemical measurements of transferrin uptake, which sample endocytosis at both the ventral and dorsal plasma membranes,

suggest a global influence of adhesion on the rate of clathrin-dependent endocytosis. Furthermore, CCP lifetimes in cells plated on fibronectin-coated coverslips were extended in regions both near and far from adhesions, supporting the idea that adhesion has a global influence on endocytosis. In contrast to our findings, Liu *et al.* (2009) found that patterned substrates, but not a uniform coating of substrate, had a global effect on endocytosis. This conflicting result may be due to the distinct culture conditions used in our two studies, including the duration of adhesion and the presence of serum. These methodological differences could have profound effects on the composition and structure of the adhesions, as well as the organization and dynamics of the actin cytoskeleton and thus differentially affect CCP dynamics.

A reduction in lamellar actin assembly and disassembly dynamics, which occurs under conditions of high adhesion (Gupton and Waterman-Storer, 2006), could also reduce the local rate of actin dynamics at sites of endocytosis. This would result in a reduction of the force that is generated for membrane deformation and thereby slow endocytosis. Finally, a reduction in actin dynamics could also prevent the endocytosis of CCPs that are embedded in the actin cytoskeleton (Gaidarov *et al.*, 1999). Thus, multiple distinct mechanisms, including physical retention of CCPs by integrins and signaling-based methods, may play roles in the regulation of endocytosis at sites of adhesion.

Contribution of Actin Dynamics to Clathrin-dependent Vesicle Formation at Sites of Adhesion

In addition to playing a negative role in CCP dynamics, actin assembly and disassembly may play a positive role in vesicle formation. However, the contribution of the actin cytoskeleton to clathrin-dependent vesicle formation remains controversial. Although actin dynamics clearly contribute to many stages of clathrin-dependent formation in some cell types and conditions (Moskowitz *et al.*, 2003; Merrifield *et al.*, 2005; Yarar *et al.*, 2005; Lee *et al.*, 2006), actin dynamics appear to play a less critical role in other cell types (Fujimoto *et al.*, 2000; Boucrot *et al.*, 2006; Liu *et al.*, 2009; Saffarian *et al.*, 2009). A previous report suggested that actin dynamics do not play a role in the formation of conventional clathrin-coated vesicles in BSC1 cells used in this study (Boucrot *et al.*, 2006). The explanation for the difference between our results and previous work may lie in the distinct experimental procedures used in the two studies, including the duration of cell attachment to the coverslip, the concentration of latrunculin B used, and the exclusion of nonproductive CCP lifetimes. We suggest that a lack of effect in vesicle formation after the disruption of actin dynamics in BSC1 cells, as previously observed, may result from a difference in inhibitor sensitivity of the cells that is dependent on the time of adhesion or a consequence of increased movement of the plasma membrane after disruption of actin assembly resulting in shorter measured CCP lifetimes.

In addition to differences in methodologies used between the many different studies, the conflicting results upon the disruption of actin dynamics found in different cell types may be accounted for by the adhesion state of the cells. Specifically, CCPs in cells with large areas of substrate adhesion or tighter local adhesion might exhibit a greater requirement for actin dynamics. In support of this model, our data reveal an increased requirement for actin assembly during clathrin-coated vesicle formation at sites of substrate adhesion.

A recent study has also suggested that actin assembly is required for the formation and uptake of flat, large clathrin structures termed "plaques" found on the adherent membrane of some cells (Saffarian *et al.*, 2009). These authors, however, did not observe these plaques in BSC1 cells, suggesting that the diffraction limited CCPs that we analyzed here are not plaques. Consistent with this, the lifetimes of our diffraction-limited CCPs at sites of adhesion are shorter (~160 s) than the lifetimes reported for the plaques (starting from ~210 s). However, because it is not clear how different culture and adhesion conditions influence the formation of plaques, we cannot rule out the possibility that the larger clathrin structures that we have observed at sites of adhesion may be related to plaques.

In summary, we propose a model in which cell–substrate adhesion increases the force required to deform a membrane during clathrin-coated vesicle formation. This mechanism is in part mediated by the direct attachment of CCP cargo, namely β1 integrin, with the ECM. This adhesion force is counteracted by actin cytoskeletal assembly, which drives vesicle formation. Interestingly, turgor pressure in budding yeast, pushing the plasma membrane against the cell wall, inhibits endocytosis, but is counteracted by actin cytoskeletal forces (Aghamohammadzadeh and Ayscough, 2009), suggesting that the mechanism underlying clathrin-mediated vesicle formation may be conserved.

ACKNOWLEDGMENTS

The authors are grateful to S. Schmid, C. Waterman, T. Parsons (University of Virginia), and R. Hynes for kindly providing reagents. We also thank S. Alford, I. Cheeseman, S. Gupton, R. Hynes, and A. Rodal for critically reading the manuscript, the Gertler lab for sharing their equipment, and the Koch Institute Microscopy core for use of the microscopes. This study was supported by a Leukemia and Lymphoma fellowship (3432-07) and a Whitehead Institute grant (D.Y.).

REFERENCES

Aggeler, J., and Werb, Z. (1982). Initial events during phagocytosis by macrophages viewed from outside and inside the cell: membrane-particle interactions and clathrin. J. Cell Biol. *94*, 613–623.

Aghamohammadzadeh, S., and Ayscough, K. R. (2009). Differential requirements for actin during yeast and mammalian endocytosis. Nat. Cell Biol. *11*, 1039–1042.

Benesch, S., Polo, S., Lai, F. P., Anderson, K. I., Stradal, T. E., Wehland, J., and Rottner, K. (2005). N-WASP deficiency impairs EGF internalization and actin assembly at clathrin-coated pits. J. Cell Sci. *118*, 3103–3115.

Blanpied, T. A., Scott, D. B., and Ehlers, M. D. (2002). Dynamics and regulation of clathrin coats at specialized endocytic zones of dendrites and spines. Neuron *36*, 435–449.

Boucrot, E., Saffarian, S., Massol, R., Kirchhausen, T., and Ehrlich, M. (2006). Role of lipids and actin in the formation of clathrin-coated pits. Exp. Cell Res. *312*, 4036–4048.

Carter, L. L., Redelmeier, T. E., Woollenweber, L. A., and Schmid, S. L. (1993). Multiple GTP-binding proteins participate in clathrin-coated vesicle-mediated endocytosis. J. Cell Biol. *120*, 37–45.

Cingolani, L. A., Thalhammer, A., Yu, L. M., Catalano, M., Ramos, T., Colicos, M. A., and Goda, Y. (2008). Activity-dependent regulation of synaptic AMPA receptor composition and abundance by beta3 integrins. Neuron *58*, 749–762.

Conner, S. D., and Schmid, S. L. (2003). Regulated portals of entry into the cell. Nature *422*, 37–44.

Curtis, A. S. (1964). The mechanism of adhesion of cells to glass. a study by interference reflection microscopy. J. Cell Biol. *20*, 199–215.

Damke, H., Baba, T., Warnock, D. E., and Schmid, S. L. (1994). Induction of mutant dynamin specifically blocks endocytic coated vesicle formation. J. Cell Biol. *127*, 915–934.

del Pozo, M. A., Balasubramanian, N., Alderson, N. B., Kiosses, W. B., Grande-Garcia, A., Anderson, R. G., and Schwartz, M. A. (2005). Phospho-caveolin-1 mediates integrin-regulated membrane domain internalization. Nat. Cell Biol. *7*, 901–908.

Ehrlich, M., Boll, W., Van Oijen, A., Hariharan, R., Chandran, K., Nibert, M. L., and Kirchhausen, T. (2004). Endocytosis by random initiation and stabilization of clathrin-coated pits. Cell *118*, 591–605.

Engqvist-Goldstein, A. E., Warren, R. A., Kessels, M. M., Keen, J. H., Heuser, J., and Drubin, D. G. (2001). The actin-binding protein Hip1R associates with clathrin during early stages of endocytosis and promotes clathrin assembly in vitro. J. Cell Biol. *154*, 1209–1223.

Fujimoto, L. M., Roth, R., Heuser, J. E., and Schmid, S. L. (2000). Actin assembly plays a variable, but not obligatory role in receptor-mediated endocytosis in mammalian cells. Traffic *1*, 161–171.

Gaidarov, I., Santini, F., Warren, R. A., and Keen, J. H. (1999). Spatial control of coated-pit dynamics in living cells. Nat. Cell Biol. *1*, 1–7.

Gupton, S. L., and Waterman-Storer, C. M. (2006). Spatiotemporal feedback between actomyosin and focal-adhesion systems optimizes rapid cell migration. Cell *125*, 1361–1374.

Hynes, R. O. (2002). Integrins: bidirectional, allosteric signaling machines. Cell *110*, 673–687.

Keyel, P. A., Watkins, S. C., and Traub, L. M. (2004). Endocytic adaptor molecules reveal an endosomal population of clathrin by total internal reflection fluorescence microscopy. J. Biol. Chem. *279*, 13190–13204.

Lee, D. W., Wu, X., Eisenberg, E., and Greene, L. E. (2006). Recruitment dynamics of GAK and auxilin to clathrin-coated pits during endocytosis. J. Cell Sci. *119*, 3502–3512.

Lenter, M., Uhlig, H., Hamann, A., Jeno, P., Imhof, B., and Vestweber, D. (1993). A monoclonal antibody against an activation epitope on mouse integrin chain beta 1 blocks adhesion of lymphocytes to the endothelial integrin alpha 6 beta 1. Proc. Natl. Acad. Sci. USA *90*, 9051–9055.

Liu, A. P., Loerke, D., Schmid, S. L., and Danuser, G. (2009). Global and local regulation of clathrin-coated pit dynamics detected on patterned substrates. Biophys. J. *97*, 1038–1047.

Loerke, D., Mettlen, M., Yarar, D., Jaqaman, K., Jaqaman, H., Danuser, G., and Schmid, S. L. (2009). Cargo and dynamin regulate clathrin-coated pit maturation. PLoS Biol. *7*, e57.

Loisel, T. P., Boujemaa, R., Pantaloni, D., and Carlier, M. F. (1999). Reconstitution of actin-based motility of *Listeria* and *Shigella* using pure proteins. Nature *401*, 613–616.

Maupin, P., and Pollard, T. D. (1983). Improved preservation and staining of HeLa cell actin filaments, clathrin-coated membranes, and other cytoplasmic structures by tannic acid-glutaraldehyde-saponin fixation. J. Cell Biol. *96*, 51–62.

Merrifield, C. J., Feldman, M. E., Wan, L., and Almers, W. (2002). Imaging actin and dynamin recruitment during invagination of single clathrin-coated pits. Nat. Cell Biol. *4*, 691–698.

Merrifield, C. J., Perrais, D., and Zenisek, D. (2005). Coupling between clathrin-coated-pit invagination, cortactin recruitment, and membrane scission observed in live cells. Cell *121*, 593–606.

Moskowitz, H. S., Heuser, J., McGraw, T. E., and Ryan, T. A. (2003). Targeted chemical disruption of clathrin function in living cells. Mol. Biol. Cell *14*, 4437–4447.

Naumanen, P., Lappalainen, P., and Hotulainen, P. (2008). Mechanisms of actin stress fibre assembly. J. Microsc. *231*, 446–454.

Rappoport, J. Z., and Simon, S. M. (2003). Real-time analysis of clathrin-mediated endocytosis during cell migration. J. Cell Sci. *116*, 847–855.

Saffarian, S., Cocucci, E., and Kirchhausen, T. (2009). Distinct dynamics of endocytic clathrin-coated pits and coated plaques. PLoS Biol. *7*, e1000191.

Schafer, D. A., Welch, M. D., Machesky, L. M., Bridgman, P. C., Meyer, S. M., and Cooper, J. A. (1998). Visualization and molecular analysis of actin assembly in living cells. J. Cell Biol. *143*, 1919–1930.

Schlunk, G., Damke, H., Kiosses, W. B., Rusk, N., Symons, M. H., Waterman-Storer, C. M., Schmid, S. L., and Schwartz, M. A. (2004). Modulation of Rac localization and function by dynamin. Mol. Biol. Cell *15*, 256–267.

Smythe, E., Redelmeier, T. E., and Schmid, S. L. (1992). Receptor-mediated endocytosis in semiintact cells. Methods Enzymol. *219*, 223–234.

Soulet, F., Yarar, D., Leonard, M., and Schmid, S. L. (2005). SNX9 regulates dynamin assembly and is required for efficient clathrin-mediated endocytosis. Mol. Biol. Cell *16*, 2058–2067.

Spector, I., Shochet, N. R., Blasberger, D., and Kashman, Y. (1989). Latrunculins—novel marine macrolides that disrupt microfilament organization and affect cell growth: I. Comparison with cytochalasin D. Cell Motil. Cytoskelet. *13*, 127–144.

van der Bliek, A. M., and Meyerowitz, E. M. (1991). Dynamin-like protein encoded by the *Drosophila* shibire gene associated with vesicular traffic. Nature *351*, 411–414.

Yarar, D., Waterman-Storer, C. M., and Schmid, S. L. (2005). A dynamic actin cytoskeleton functions at multiple stages of clathrin-mediated endocytosis. Mol. Biol. Cell *16*, 964–975.